T. Takaki, A. Yamanaka and Y. Tomita / Proceedings, AES – ATEMA' 2007 International Conference, Montreal, Canada, August 06 -10, 2007, pp. 223 - 231

ISBN 0-9780479

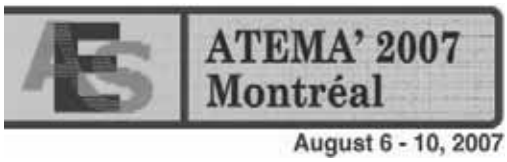

International Conference on Advances and Trends in Engineering Materials and their Applications (AES – ATEMA' 2007)

Phase-Field Modeling for Dynamic Recrystallization

T. Takaki [1]*, A. Yamanaka [2], Y. Tomita [3]

[1] Faculty of Maritime Sciences, Kobe University, 5-1-1, Fukaeminami, Higashinada, Kobe, 658-0022, Japan
(Email: takaki@maritime.kobe-u.ac.jp)

[2] Graduate School of Science and Technology, Kobe University, 1-1, Rokkodai, Nada, Kobe, 657-8501, Japan
(Email: yamanaka@solid.mech.kobe-u.ac.jp)

[3] Faculty of Engineering, Kobe University, 1-1, Rokkodai, Nada, Kobe, 657-8501, Japan
(Email: tomita@mech.kobe-u.ac.jp)

*Corresponding Author

Abstract

Dynamic recrystallization (DRX) exhibits very complicated phenomena including both hardening due to the accumulation of dislocations and softening due to the nucleation and growth of recrystallized grains. In other words, the mechanical behaviour during the DRX process is closely related to the evolution of microstructures and dislocations. In this study, the phase-field model, which enables the simulation of microstructural variation during the DRX process, is developed by generalizing the multi-phase-field method proposed by Steinbach et al. The hardening due to the accumulation of dislocations and the nucleation criteria of recrystallization are expressed theoretically by employing the method proposed by Guo et al. In order to confirm the basic performance of the developed model, a simulation of single-grain growth is performed. As a result, the characteristic variation of the grain boundary migration rate due to the dislocation-density change and a good agreement with the theoretical result were observed. Furthermore, the DRX process including nucleation is simulated for a regular-hexagonal grain structure. It is confirmed that a typical stress – strain curve with multiple peaks can be reproduced by the prediction of microstructural evolution.

Keywords

Phase-Field Method, Modeling, Simulation, Dynamic Recrystallization, Microstructure Evolution, Dislocation.

1 Introduction

It is well known that when a low-to-medium stacking fault energy (SFE) metal is deformed under a high-temperature environment, dynamic recrystallization (DRX) occurs [1, 2]. DRX is distinguished from static recrystallization (SRX), which occurs in post-deformation annealing. Although both recrystallization processes have many common characteristics, the most different point is that for DRX, the dislocation density in the recrystallized grains increases with continuous deformation, while for SRX, it is constant. Since DRX exhibits complicated phenomena such as hardening due to deformation and softening due to recrystallized grain growth, or the simultaneous evolution of dislocations and microstructures over time, the construction of a numerical model that enables the evaluation of microstructural evolution is essential, in addition to experimental observation.

As a numerical model for DRX, the cellular automaton (CA) method [3-9] has been successfully applied to the microstructural investigation of the DRX process. Guo et al. [7-9] have proposed a simulation method that couples the CA method to a theoretical model, in which the hardening by the accumulation of dislocations is expressed by equations and the softening by grain boundary migration due to recrystallization is simulated by the CA method. However, since the CA method describes the states in terms of discrete variables, it is problematic when applied to modeling curvature-driven growth [10].

The phase-field method was first used to model dendrite formation [11, 12], and over the past decade, it has been applied to various problems of material science. The phase-field method can easily reproduce complicated shapes and morphologies without tracking the location of the interface, since the interface migration is described by the time evolution of an additional order parameter, or the phase field. In this model, the time and scale can be treated as the real values, and the effect of curvature is explicitly included.

In this study, we establish a phase-field model for the DRX process, in which the multi-phase-field method proposed by Steinbach et al. [14] is generalized to simulate the grain boundary migration driven by stored energy, or the softening process. The hardening process is modeled by the equations employed by Guo et al. [6, 7].

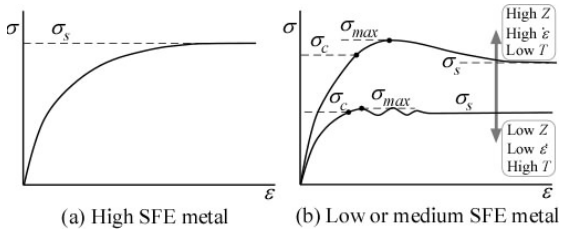

Figure 1. Schematic stress-strain curves under hot working.

2 Dynamic Recrystallization

Figure 1 schematically illustrates typical stress-strain curves under hot working. In metals with a high-SFE, such as Al and α-Fe, the stress increases monotonically with increasing strain, because the dynamic recovery is rapid and the dislocation density does not achieve a critical value that originates the nucleation of recrystallization. On the other hand, the low- or medium-SFE metals, such as Cu, Ni and γ-Fe, exhibit DRX. The stress-strain curve for the low- or medium-SFE metals is characterized by the Zener-Holloman parameter Z, defined by the following equation:

$$Z = \dot{\varepsilon}\exp(Q/RT), \quad (1)$$

where $\dot{\varepsilon}$ is the strain rate, T is the deformation temperature, Q is the activation energy and R is the gas constant. As shown in Fig. 1 (b), under the conditions of low Z, i.e., low $\dot{\varepsilon}$ or high T, the stress-strain curve has multiple peaks at low strain, and under high Z, i.e., high $\dot{\varepsilon}$ or low T, it exhibits a single peak. For both cases, when the stress attains a critical value σ_c which is somewhat less than the maximum stress σ_{max}, the nucleation of recrystallization is generated. Since the dislocation density of the recrystallized grain is considerably smaller than that of the deformed material, softening occurs with the growth of the new grain. Finally, the steady-state stress σ_s is achieved.

3 Theoretical Model

We employ the model of dislocation evolution and nucleation used in Refs. [6] and [7].

3.1 Dislocation evolution model

The variation of the dislocation density ρ with respect to the strain ε is given by

$$\frac{d\rho}{d\varepsilon} = k_1\sqrt{\rho} - k_2\rho . \quad (2)$$

Here, the first term of the right hand side expresses the work hardening, and k_1 is a constant that represents hardening. The second term is the dynamic recovery term, and k_2 is a function of temperature T and strain rate $\dot{\varepsilon}$. The flow stress σ is related to the dislocation density as follows:

$$\sigma = \alpha\mu\tilde{b}\sqrt{\rho}, \quad (3)$$

where α is a dislocation interaction coefficient of around 0.5, μ is the shear modulus, and $\tilde{b}$ is the magnitude of the Burgers vector.

In our numerical model, the local dislocation evolution is expressed by Eq. 2, and the macroscopic true stress is calculated from Eq. 3 by changing ρ to an average dislocation density ρ_{ave} over a numerical region.

The following formulations are performed in order to identify k_1 and k_2 in Eq. 2. From Eqs. 2 and 3, we can obtain the following equation,

$$\frac{d\sigma}{d\varepsilon} = \frac{1}{2}\alpha\mu\tilde{b}k_1\left(1 - \frac{\sigma}{\sigma_s}\right) \quad (4)$$

where σ_s is the steady-state stress and is expressed as

$$\sigma_s = \alpha\mu\tilde{b}k_1/k_2 \quad (5)$$

From the gradient of the stress-strain curve at $\sigma = 0$, k_1 can be determined. The steady-state stress σ_s is related to the strain rate $\dot{\varepsilon}$ and temperature T as

$$\dot{\varepsilon} = A\sigma_s^m \exp\left(-\frac{Q_{act}}{RT}\right) \quad (6)$$

where A and m are constants and Q_{act} is the activation energy. When σ_s is determined from Eq. 6, k_2 can be obtained from Eq. 5.

$$k_2 = \alpha\mu\tilde{b}k_1/\sigma_s \quad (7)$$

3.2 Nucleation model

Since the nucleation originates at high-angle boundaries, it is assumed that the nucleation of DRX only occurs at the original and recrystallized grain boundaries. In this case, the nucleation mechanism reduces to bulging nucleation. Considering that the nucleation originates when the dislocation density reaches a critical value ρ_c, ρ_c can be calculated on the basis of the bulging mechanism as follows [13]:

$$\rho_c = \left(\frac{20\gamma\dot{\varepsilon}}{3\tilde{b}LM\tau^2}\right)^{1/3}, \quad (8)$$

where γ is the grain boundary energy, L is the mean free path of the dislocation, M is the grain boundary mobility and τ is the dislocation line energy calculated by $\tau = c\mu\tilde{b}^2$, in which c is a constant of the order of 0.5. The mean free path L is calculated from $L = K/\alpha\sqrt{\rho}$, where K is a constant of about 10.

4 Phase-Field Model

4.1 Phase-field equations for DRX

We generalize the multi-phase-field model proposed by Steinbach et al. [14] to simulate the DRX phenomenon, in which the recrystallized grain boundary migration is driven by the stored energy.

We consider a system containing N different grains ϕ_1, ϕ_2, ...ϕ_N. Phase field ϕ_α takes a value of 1 inside the αth grain, and is 0 inside other grains, and $0 < \phi_\alpha < 1$ at the grain boundary. ϕ_α is not an independent variable and must satisfy following condition:

$$\sum_{\alpha=1}^{N} \phi_\alpha = 1 . \tag{9}$$

Here, we use the free-energy functional

$$\begin{aligned} F &= \int_V f dV \\ &= \int_V \left[\sum_{\alpha=1}^{N} \sum_{\beta=\alpha+1}^{N} \left(-\frac{a_{\alpha\beta}^2}{2} \nabla\phi_\alpha \cdot \nabla\phi_\beta + W_{\alpha\beta}\phi_\alpha\phi_\beta \right) + f_e \right] dV \end{aligned} , \tag{10}$$

where $a_{\alpha\beta}$ and $W_{\alpha\beta}$ are the gradient coefficient and the barrier height, respectively, which are related to the interface energy γ_{ij} and the interface thickness δ_{ij}. f_e is the bulk free-energy density and a function of ϕ_1, ϕ_2, ...ϕ_N, i.e., $f_e = f_e(\phi_1, \phi_2, \cdots \phi_N)$.

Now, we define a step function σ_a as

$$\sigma_\alpha = \begin{cases} 1 \cdots 0 < \phi_\alpha < 1 \\ 0 \cdots \text{elsewhere} \end{cases} . \tag{11}$$

Using this step function, the number of locally present phases is expressed as

$$n = \sum_{\alpha=1}^{N} \sigma_\alpha(x,t) . \tag{12}$$

Using Eq. 12, Eq. 9 reduces to

$$\sum_{i=1}^{n} \phi_i = 1 . \tag{13}$$

By introducing the Lagrange multiplier λ, ϕ_1, ϕ_2, ...ϕ_N can be treated as independent variables.

$$\Gamma = F + \int_V \left\{ \lambda \left(\sum_{i=1}^{n} \phi_i - 1 \right) \right\} dV \tag{14}$$

Since ϕ_i is a non-conserved order parameter, the time evolution equation of ϕ_i can be expressed as follows:

$$\overset{\circ}{\phi}_i = -\frac{\delta F}{\delta \phi_i} - \lambda , \tag{15}$$

where $\overset{\circ}{\phi}_i$ denotes the time evolution without considering a specific time scale.

Furthermore, an interface field ψ_{ij} is newly defined as follows:

$$\psi_{ij} = \phi_i - \phi_j \quad (i < j), \tag{16}$$

where $\psi_{ij} = -\psi_{ij}$. Substituting Eq. 16 into Eq. 13, we obtain

$$\phi_i = \frac{1}{n} \left(\sum_{j=1}^{n} \psi_{ij} + 1 \right) . \tag{17}$$

By the definition of the interface field ψ_{ij}, or using Eq. 16, the time evolution of ψ_{ij} becomes

$$\overset{\circ}{\psi}_{ij} = \overset{\circ}{\phi}_i - \overset{\circ}{\phi}_j = -\frac{\delta F}{\delta \phi_i} + \frac{\delta F}{\delta \phi_j} . \tag{18}$$

We can see from Eq. 18 that the time evolution of ψ_{ij} is independent of the Lagrange multiplier λ. From Eq. 17,

$$\overset{\circ}{\phi}_i = \frac{1}{n} \sum_{j=1}^{n} \overset{\circ}{\psi}_{ij} . \tag{19}$$

Substituting Eq. 18 into Eq. 19, we have

$$\overset{\circ}{\phi}_i = -\frac{1}{n} \sum_{j=1}^{n} \left(\frac{\delta F}{\delta \phi_i} - \frac{\delta F}{\delta \phi_j} \right) . \tag{20}$$

The functional derivative $\delta F / \delta \phi_i$ is calculated as

$$\begin{aligned} \frac{\delta F}{\delta \phi_i} &= \frac{\partial f}{\partial \phi_i} - \nabla \frac{\partial f}{\partial \nabla \phi_i} \\ &= \sum_{\substack{k=1 \\ (k \neq i)}}^{n} \left(W_{ik}\phi_k + \frac{a_{ik}^2}{2} \nabla^2 \phi_k \right) + \frac{\partial f_e}{\partial \phi_i} \end{aligned} . \tag{21}$$

Taking into account Eq. 21 and the mobility M_{ij}^{ϕ}, the time evolution equation of ϕ_i is obtained as

$$\dot{\phi}_i = -\sum_{j=1}^{n} \frac{M_{ij}^{\phi}}{n}\left(\frac{\delta F}{\delta \phi_i} - \frac{\delta F}{\delta \phi_j}\right) = -\sum_{j=1}^{n} \frac{M_{ij}^{\phi}}{n}\left[\sum_{k=1}^{n}\left\{\left(W_{ik} - W_{jk}\right)\phi_k + \frac{1}{2}\left(a_{ik}^2 - a_{jk}^2\right)\nabla^2\phi_k\right\} + \left(\frac{\partial f_e}{\partial \phi_i} - \frac{\partial f_e}{\partial \phi_j}\right)\right] \quad (22)$$

Here, we select

$$\frac{\partial f_e}{\partial \phi_i} - \frac{\partial f_e}{\partial \phi_j} = -\frac{8}{\pi}\sqrt{\phi_i \phi_j}\,\Delta E_{ij}, \quad (23)$$

where ΔE_{ij} is the difference in bulk free-energy density between grains i and j. The factor $8/\pi$ is needed to satisfy $8/\pi \int_0^1 \sqrt{\phi(1-\phi)}\,d\phi = 1$. Finally, we obtain

$$\dot{\phi}_i = -\sum_{j=1}^{n} \frac{M_{ij}^{\phi}}{n}\left[\begin{array}{l}\displaystyle\sum_{k=1}^{n}\left\{\left(W_{ik} - W_{jk}\right)\phi_k + \frac{1}{2}\left(a_{ik}^2 - a_{jk}^2\right)\nabla^2\phi_k\right\} \\ \displaystyle -\frac{8}{\pi}\sqrt{\phi_i \phi_j}\,\Delta E_{ij}\end{array}\right]. \quad (24)$$

4.2 Phase-field parameters

The parameters a_{ij}, W_{ij} and M^{ϕ}_{ij} in Eq. 24 are related to the material constants. Let us consider the case of $N = 2$ and $n = 2$. For $\phi_1 = \phi$, $\phi_2 = 1-\phi$, $a = a_{12} = a_{21}$, $W = W_{12} = W_{21}$, $M^{\phi} = M^{\phi}_{12}$ and $\Delta E = \Delta E_{12}$, the time evolution equation of $\phi_1 = \phi$ is written as

$$\dot{\phi} = \frac{M^{\phi}}{2}\left[a^2\nabla^2\phi - W(1-2\phi) + \frac{8}{\pi}\sqrt{\phi(1-\phi)}\,\Delta E\right]. \quad (25)$$

In same way, from Eq. 10, we obtain

$$F = \int\left\{\frac{a^2}{2}(\nabla\phi)^2 + W\phi(1-\phi) + f_e\right\}dV. \quad (26)$$

In a one-dimensional problem, Eqs. 25 and 26 respectively reduce to

$$\dot{\phi} = \frac{M^{\phi}}{2}\left[a^2\frac{\partial^2\phi}{\partial x^2} - W(1-2\phi) + \frac{8}{\pi}\sqrt{\phi(1-\phi)}\,\Delta E\right] \quad (27)$$

$$F = \int\left\{\frac{a^2}{2}\left(\frac{\partial\phi}{\partial x}\right)^2 + W\phi(1-\phi) + f_e\right\}dV. \quad (28)$$

From Eq. 27, the phase-field profile under the equilibrium condition can be obtained by setting $\dot{\phi} = 0$ and $\Delta E = 0$ as follows:

$$\phi = \frac{1}{2}\left[1 - \sin\left(\frac{\sqrt{2W}}{a}x\right)\right], \quad (29)$$

where $\phi = 1/2$ at $x = 0$. Solving Eq. 29 for x,

$$x = \frac{a}{\sqrt{2W}}\sin^{-1}(-2\phi + 1). \quad (30)$$

Since the interface region is $0 < \phi < 1$, the interface thickness δ is calculated as

$$\delta = \frac{a\pi}{\sqrt{2W}}. \quad (31)$$

The grain boundary energy γ is obtained from Eq. 28 by setting $f_e = 0$ as

$$\gamma = \frac{a\sqrt{W}}{4\sqrt{2}}\pi. \quad (32)$$

Considering the condition that a grain boundary with the equilibrium phase-field profile migrates with a constant velocity V, we obtain following equation from Eq. 27:

$$V = M^{\phi}\frac{4a}{\pi\sqrt{2W}}\Delta E. \quad (33)$$

Comparing Eq. 33 and the grain boundary mobility M,

$$M = M^{\phi}\frac{4a}{\pi\sqrt{2W}}. \quad (34)$$

From Eqs. 31, 32 and 34, the phase-field parameters are related to the material parameters as follows:

$$W = \frac{4\gamma}{\delta},\quad a = \frac{2}{\pi}\sqrt{2\delta\gamma},\quad M^{\phi} = \frac{\pi^2}{4\delta}M. \quad (35)$$

Generalizing Eq. 35 to the multi grain problem,

$$W_{ij} = \frac{4\gamma_{ij}}{\delta},\quad a_{ij} = \frac{2}{\pi}\sqrt{2\delta\gamma_{ij}},\quad M^{\phi}_{ij} = \frac{\pi^2}{4\delta}M_{ij}. \quad (36)$$

where $a_{ij} = a_{ji}$, $W_{ij} = W_{ji}$, $M^{\phi}_{ij} = M^{\phi}_{ji}$, $\gamma_{ij} = \gamma_{ji}$ and $M_{ij} = M_{ji}$, and we set $\delta_{ij} = \delta$.

The driving force of the migration of the recrystallized grain boundary is expressed by the dislocation density difference between grains i and j, or

$$\Delta E_{ij} = \tau(\rho_j - \rho_i), \quad (37)$$

where $\Delta E_{ij} = -\Delta E_{ji}$. The dislocation density increases with continuous deformation by Eq. 2.

When nucleation occurs, the dislocation density in the new grain is set to an initial value ρ_0. We assume that the dislocation density in a grain is uniform, i.e., ρ_i is uniformly distributed in the region of $\phi_i > 0$ and $\rho_i = \rho_0$ when $\phi = 0$.

5 Numerical Results

On the basis of Refs. [15] and [7], we employ the following material parameters for OFHC copper: $\alpha = 0.5$, $\mu = 42.1$ GPa, $\tilde{b} = 0.256$ nm, $A = 2.78\times10^{-45}$, $m = 7.58$, $Q_{act} = 261$ KJ/mol, $R = 8.314$ J/mol·K, $k_1 = 3.71\times10^{8}$ 1/m, $\gamma = 0.625$ J/m^2, $c = 0.5$ and $K = 10$. The grain boundary mobility M is expressed by

$$M = \frac{\tilde{b}\,\delta_b D}{kT}\exp\left(-\frac{Q_b}{RT}\right), \tag{38}$$

where δ_b is the characteristic grain boundary thickness, D is the boundary self-diffusion coefficient, k is the Boltzmann constant and Q_b is the boundary diffusion activation energy. We use $\delta_b D = 5.0\times10^{-15}$ m^3/s, $k = 1.381\times10^{-23}$ J/K and $Q_b = 104$ KJ/mol [7].

Equation 24 is solved by the finite difference method, and the grid size $\Delta x = 5$ μm and the interface thickness $\delta = 7\Delta x$ are employed. The simulations are carried out under $T = 775$ K, $\dot{\varepsilon} = 2\times10^{-3}$ 1/s, and $\rho_0 = 10^9$ 1/m^2.

5.1 Single-grain growth

During the DRX process, the driving force of grain boundary migration changes with continuous deformation. Here, we perform fundamental simulations in which one recrystallized grain grows in a deformed material with a crystal orientation, and we compare numerical and theoretical results to clarify the validity of the proposed phase-field model for DRX.

A nucleus is placed at the origin of the square numerical model. The radius of the nucleus is set to $R_0 = 5.5$ μm, because it must satisfy $R_0 > \gamma/E_c$ to avoid the shrinking of the grain due to the curvature effect. The critical dislocation density ρ_c calculated by Eq. 8 is 8.82×10^{14} 1/m^2, then, the stored energy $E_c = 0.12$ MPa. Figure 2 shows the variation of grain boundary migration velocity with time. The result denoted by a broken line is for a constant stored energy E_c. This corresponds to the SRX process. In this case, the velocity is slow at the beginning of the growth due to the curvature effect then gradually become faster. On the other hand, the result for DRX indicates a peak velocity at approximately 18 s. Figure 3 shows the variation of dislocation densities in the deformed material and recrystallized grain, and the driving pressure with time. It can be observed that the dislocation density in the deformed material increases slightly, whereas that in the recrystallized grain increases rapidly from ρ_0. Consequently, the driving pressure calculated by the difference in the dislocation densities also reaches a peak. At the balance between the driving pressure and the curvature effect, the peak value of the migration velocity is determined. The solid circles in Fig. 2 indicate the theoretical values calculated from $V = M(\Delta E_{store} - \gamma/R)$. It is, therefore, confirmed that the numerical result perfectly agrees with the theoretical value.

5.1 Multi grain nucleation and growth

The DRX simulation for a polycrystal metal with regular hexagonal grains and a mean grain size is 78 μm is performed here. The size of the computational domain is 223.5×129.0 μm (447×258 grid) and the number of original grains is six. Periodic boundary conditions are employed at all boundaries.

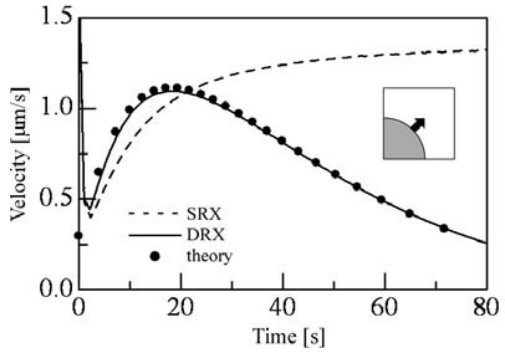

Figure 2. Variations of grain boundary migration velocity with time.

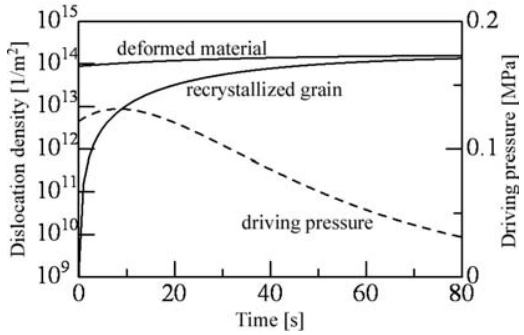

Figure 3. Variations of dislocation densities and driving pressure with time.

First, a preliminary calculation is carried out to create the initial polycrystal structure. Figure 4 shows time slices during the preliminary calculation. The six nuclei are placed in the calculated positions and grow inside a base material driven by a uniform driving force. Since the grain boundary energies are all identical, six regular-hexagonal grains can be obtained.

The DRX simulation considering nucleation is performed using the created regular-hexagonal grain structure. The nuclei are generated on the grid satisfying the conditions $\rho > \rho_c$ and $\sum_{i=1}^{n} \phi_i^2 < 0.6$. The nucleation rate is assumed to be 22.2 /s in the computational area. Here, as mentioned in the previous section, the required size of the nucleus is much larger than that of an actual nucleus. Therefore, we use $M_\phi = M_\phi/4$ and $E_{store} = 4\ E_{store}$ at all points and set the radius of the nuclei to $R_0 = 5\Delta x$. Figure 5 demonstrates the time evolution of the microstructure. When the dislocation density reaches the critical value ρ_c, the recrystallized grains are nucleated at the grain boundaries and grow toward the center of the original grains. Figure 6 shows the variation of dislocation densities with the progress of deformation. It can be seen that the dislocation density inside the recrystallized grains is lower than that in the original grains and increases with the continuous deformation. The stress – strain curves are illustrated in Fig. 7. The broken line shows the result obtained using Eqs. 2 and 3 and the solid line shows the present result. The open circles in Fig. 7 correspond to those in Figs. 5 and 6. We can observe typical multiple peaks caused by the softening due to the growth of recrystallized grains and the hardening due to the accumulation of dislocations. As a result, it is concluded that the developed phase-field model can simulate the DRX process including the softening and hardening.

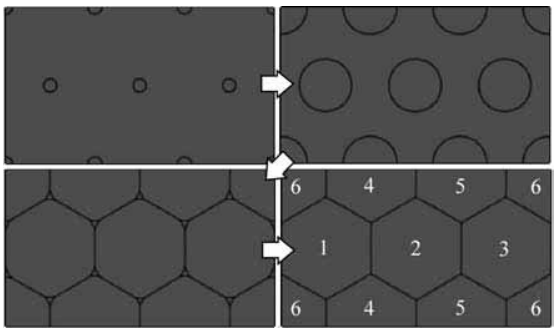

Figure 4. Time slices during computation to create initial polycrystal structure.

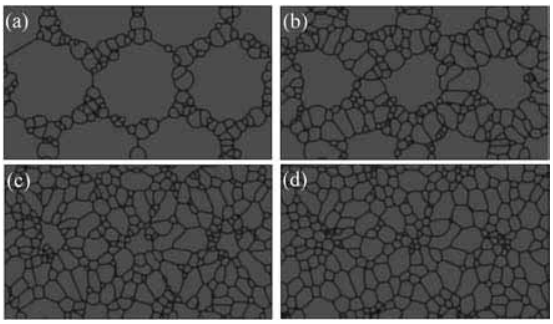

Figure 5. Microstructure evolutions ε = (a) 0.102, (b) 0.114, (c) 0.126 and (d) 0.138.

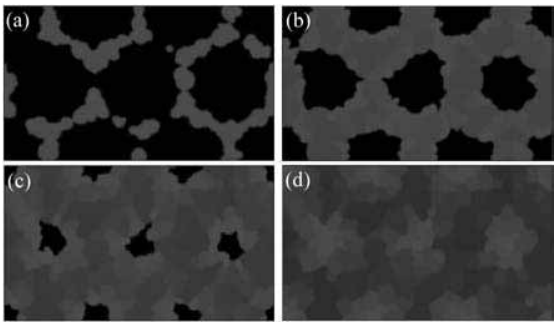

Figure 6. Variations of dislocation density.

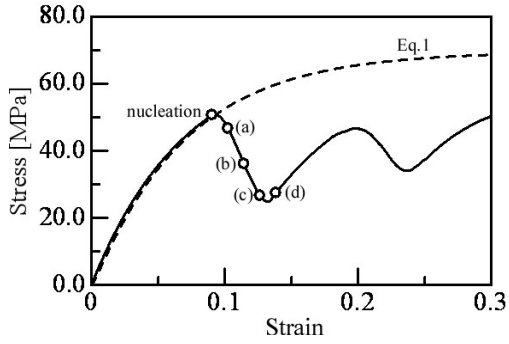

Figure 7. Stress-strain curves.

6 Conclusions

We have established a phase-field model for the DRX process, in which the multi-phase-field method proposed by Steinbach et al. was generalized to simulate the grain boundary migration driven by stored energy. The hardening was modeled using the theoretical equations employed by Guo et al. The basic single-grain growth and the DRX process resulting from the regular hexagonal grain structure were simulated. It was confirmed that the developed phase-field model can simulate the DRX process.

Acknowledgement

This research was partially supported by the Ministry of Education, Culture, Sports, Science and Technology Grant-in-Aid for Scientific Research (B), 18360061, 2007.

References

[1] Sakai, T., Jonas, J. J., (1984) Dynamic recrystallization: Mechanical and microstructural considerations, *Acta Metall.*, 32 (2), 189–209.

[2] Humphreys, F. J., Hatherly, M. (2004) *Recrystallization and Related Annealing Phenomena*, Elsevier.

[3] Goetz, R. L., Seetharaman, V., (1998) Modeling dynamic recrystallization using cellular automata, *Scr. Mate.,* 38 (3), 405–413.

[4] Goetz, R. L., (2005) Particle stimulated nucleation during dynamic recrystallization using a cellular automata model, *Scr. Mate.*, 52, 851–856.

[5] Goetz, R. L., (2005) Particle stimulated nucleation during dynamic recrystallization using a cellular automata model, *Scr. Mate.*, 52, 851–856.

[6] Kugler, G., Turk, R., (2004) Modeling the dynamic recrystallization under multi-stage hot deformation, *Acta Mater.*, 52, 4659–4668.

[7] Ding, R., Guo, Z. X., (2001) Coupled quantitative simulation of microstructural evolution and plastic flow during dynamic recrystallization, *Acta Mater.*, 49, 3163–3175.

[8] Ding, R., Guo, Z. X., (2004), Microstructural evolution of a Ti-6Al-4V alloy during b-phase processing: experimental and simulative investigations, *Mater. Sci. Eng. A*, 365, 172–179.

[9] Qian, M., Guo, Z. X., (2004) Cellular automata simulation of microstructural evolution during dynamic recrystallization of an HY-100 steel, *Mater. Sci. Eng. A*, 365, 180–185.

[10] Miodownik, M. A., (2002) A review of microstructural computer models used to simulate grain growth and recrystallisation in aluminium alloys, *J. Light Metals*, 2, 125–135.

[11] Kobayashi, R., (1993) Modeling and numerical simulations of dendritic crystal growth, *Physica D*, 63 (3-4). 410–423.

[12] Warren, J.A., Boettinger, W.J., (1995) Prediction of dendritic growth and microsegregation patterns in a binary alloy using the phase-field method, *Acta Metall.*, 43 (2), 689–703.

[13] Roberts, W., Ahlblom, B., (1978) A nucleation criterion for dynamic recrystallization during hot working, *Acta Metal.*, 26, 801–813.

[14] Steinbach, I., Pezzolla, F., (1999) A generalized field method for multiphase transformations using interface fields, *Physica D*, 134, 385–393.

[15] Blaz, L., Sakai, T., Jonas, J. J., (1983) Effect of initial grain size on dynamic recrystallization of copper, *Metal Science*, 17, 609–616.